

### ANTIMICROBIAL EFFECT OF SILVER NANOPARTICLE-BASED THIN FILMS

Miroslav Rajnec<sup>\*1,5</sup>, Marek Vidiš<sup>2</sup>, Marián Tomka<sup>3</sup>, Mária Šedivá<sup>1</sup>, Andrea Gažiová<sup>4</sup>, Ján Mucha<sup>1</sup>

Address(es): Ing. Miroslav Rajnec, PhD.

<sup>1</sup> Institute of Chemistry SAS, Center of Glycomics, Dúbravská cesta 9, Bratislava 84538, Slovakia.

<sup>2</sup> Comenius University, Faculty of Mathematics, Physics and Informatics, Turany 1148, 03853 Turany, Slovakia.

<sup>3</sup> Slovak University of Agriculture in Nitra, Faculty of Biotechnology and Food Sciences, Institute of Biotechnology, Trieda Andreja Hlinku 2, Nitra 94976, Slovakia.

<sup>4</sup> Public Health Authority of the Slovak Republic, Trnavská cesta 52, 82645 Bratislava, Slovakia.

<sup>5</sup> Institute of Plant Genetics and Biotechnology, Plant Science Biodiversity Center, Slovak Academy of Sciences, Akademická 2, 950 07 Nitra, Slovak Republic.

\*Corresponding author: [rajnec.miroslav@gmail.com](mailto:rajnec.miroslav@gmail.com)

<https://doi.org/10.55251/jmbfs.10073>

#### ARTICLE INFO

Received 16. 4. 2023

Revised 14. 5. 2023

Accepted 16. 5. 2023

Published 1. 6. 2023

Regular article



#### ABSTRACT

The global pandemic of disease COVID-19 caused by the pathogenic SARS-Cov-2 virus brought more interest in the public health community for known silver with its potential antimicrobial properties to fight infection. One of the ways to stop virus to protect community transmission is the application of nanotechnology of silver nanoparticles on the exposed surfaces of daily used materials in public, e.g., transportation, community spaces, hospitals, and everywhere where the potential infection load is increased. Published technology to coat AgNPs on surfaces differs in the preparation of nanocomposites and substrates, which results in different mechanical and antimicrobial properties. In our study, we focused on the properties of AgNPs prepared by HiTUS and PVD technology with a challenge to test the antimicrobial effect towards the model of gram-negative bacteria (*Escherichia coli*), fungi (*Trichoderma harzianum*) and related enteroviruses (*Poliovirus* and *Coxsackie*). All tested materials showed 59% or more growth inhibition of *E. coli*. Growth of *T. harzianum* was inhibited by 16% in the presence of AgTiB<sub>2</sub> 50W, and other materials caused 37% to 68% inhibition. Enteroviruses infection was completely inhibited after 1 hour of AgNPs treatment. Only *Coxsackie* A7 retained infection capability after 30 minutes of treatment with AgNPs. Moreover, the ICP-OES-measured amounts of silver released in cultivation media are lower than most published studies of silver nanoparticles with a comparable antimicrobial effect. Keeping silver concentration at the lowest possible limit is one of the most critical factors for producing environmentally safe antimicrobial materials for everyday use.

**Keywords:** AgNPs, silver nanoparticle-based thin films, antimicrobial effect

#### INTRODUCTION

The evolution of nanotechnology in the last few decades can be described as one of the most effective tools for the production of nanomaterials with significant potential impact in the field of manufacturing output, treatment of illnesses, remediation of the environment, and control of microscopic biological pathogens and pests (MacCormack and Goss, 2008). Most nanomaterials used in final commercial products are based on metal nanoparticles of Ag, Ti, Zn, Au, Se, or Cu. The main advantage of using nanoparticle technology lies in the increased ratio of large surface area to volume, which leads to higher reactivity and often different optical, mechanical, electrical, magnetic, and biological properties in comparison with their solid macro material counterparts (Fubini et al., 2011).

Silver nanoparticles (AgNPs) have been well studied for their promising antimicrobial effect and they are currently among the most widely used metallic nanoparticles. Pathogenic microorganisms, such as bacteria, viruses, and fungi, are negatively affected in the presence of silver. When AgNPs are compared to their solid form, an immense larger surface area is a feature that leads to better contact with microorganisms and, thus, higher biocidal activity (Kalwar and Shan, 2018). Today, AgNPs are successfully used in more than 300 consumer products, mainly when an antiseptic and antimicrobial effect is particularly desirable. Their use includes electronics, textiles, cosmetology, pharmacy, and medicine (Dorobantu et al., 2015).

The specific mechanism of the antibacterial activity of AgNPs has not yet been completely explained. Releasing of Ag<sup>+</sup> ions is often considered one of the mechanisms of the antibacterial activity of AgNPs. Silver ions form complexes with nucleic acids and interact specifically with nucleotides. Interactions with sulfur proteins and electrostatic attraction to negatively charged microbial cells allow the adhesion of AgNPs to the cytoplasm and cell wall, enhancing permeability and disrupting bacterial cells (Cao et al., 2001). When Ag<sup>+</sup> ions enter the cell cytoplasm, the respiratory enzyme system is deactivated, producing reactive oxygen species (ROS). AgNPs also hinder protein synthesis by denaturation of cytoplasmic ribosomal components (Pareek et al., 2018) and trigger the denaturation of cell membranes (Liao et al., 2019). Inhibition of protein and cell wall synthesis caused by AgNPs leads to ATP leakage and apoptosis (Anees Ahmad et al., 2020). The main factors which influence the physiological

properties of AgNPs include their size, morphology, surface, and distribution in prepared material. These can be altered by stabilizers, reducing agents, and synthesis method (Carlson et al., 2008).

Nanoparticles can be produced by the “bottom-up” approach, where nanoparticles are formed by the self-assembly of atoms. They are produced by vapor deposition, laser pyrolysis, aerosol processes, and by biosynthesis in plants, fungi, yeast, and bacteria. The “top-down” approach of nanoparticles production is based on the size reduction of larger particles with equipment capable of material removal from “bulk” to form nanosized range structures. Techniques like mechanical milling, sputtering, chemical etching, and laser ablation are used (Slepička et al., 2020). Both approaches have their advantages and disadvantages. The main selling point of “bottom-up” techniques is using of environmentally friendlier solvents. The potential for the “top-down” approach comes in producing protection equipment susceptible to microbial or viral colonization (Jadoun et al., 2022).

COVID-19 pandemic brings questions about possible ways to slow down the contagion or completely avoid the disease transmission in the population. Equipment like facial masks, filters for air conditioning systems, or heavily exposed surfaces, like door handles or water taps, are ideal candidates for AgNPs antimicrobial protection (Balagna et al., 2020).

The use of AgNPs brings a couple of issues highly discussed in the scientific community involving their toxicity and environmental impact. They can be seen as an eco-toxic biodegradable threat or a material bio-accumulating in the trophic chain. Today, the amount of produced nanomaterials with silver content is challenging to estimate. Still, it is clear that if silver content in products is not carefully monitored and regulated, the risk of environmental threats caused by a massive increase in its concentration increases (Pulit-Prociak and Banach, 2016). The objective of our study was to evaluate the antimicrobial effect of AgNPs prepared by two methods of the “top-down” approach, HiTUS - High Target Utilization Sputtering and PVD - Physical Vapor Deposition of the complex of Ag and TiB<sub>2</sub> (Izai et al., 2023). The Inductively Coupled Plasma Optical Emission Spectroscopy (ICP-OES) method was used to measure released silver ions from AgNPs coating to determine released silver ions from AgNPs coating for the determination of released Ag concentration at the tested conditions to figure out a possible toxic impact on the environment. Prepared AgNPs coated on Si substrate

were tested against model organisms of bacteria (*E. coli*), microscopic filamentous fungi (*T. harzianum*), and enteroviruses (*Poliovirus* and *Coxsackie*).

## MATERIAL AND METHODS

### Silver nanoparticles

AgNPs were prepared by two different methods, HiTUS and PVD, and immobilized on a silica plate with a 5 x 8 x 0.5 mm dimension. Parameters of preparation and Ag concentration in atomic percent (at. %) are listed in Table 1.

**Table 1** Technology of production and immobilization of AgNPs on silica plates

Sample	Ag concentration [at. %]	Technology	Parameters
Ag-TiB <sub>2</sub> 50W	9.34		Ag 50W, TiB <sub>2</sub> 1000W, bias = -60V
Ag-TiB <sub>2</sub> 100W	16.9	Physical Vapor Deposition	Ag 100W, TiB <sub>2</sub> 1000W, bias = -60V
Ag-TiB <sub>2</sub> 200W	28.4		Ag 200W, TiB <sub>2</sub> 1000W, bias = -60V
Ag1	40		500W, 0.2 Pa, Ub = 0W, 10 min
Ag5	57	High Target Utilization Sputtering	500W, 0.1 Pa, Ub = 0W, 10 min
Ag6	16		500W, 0.5 Pa, Ub = 0W, 10 min

**Legend:** at.% - atomic percent; TiB<sub>2</sub> - titanium diboride; Ub - bias of holder

### Bacterial, fungal, virus strains and cultivation conditions

Gram-negative bacteria *Escherichia coli* DH5aF' (Woodcock et al., 1989) was cultivated in liquid lysogeny broth [1% (w/v) peptone; 0.5% (w/v) yeast extract; 1.5% (w/v) NaCl] at 37 ± 1 °C with shaking at 180 rpm overnight. The overnight culture was transferred into fresh LB and cultivated until OD<sub>600</sub> 0.08 – 0.12 (0.5 McFarland Units – MFU).

Microscopic filamentous fungi *Trichoderma harzianum* CCM F-340 (Czech Collection of Microorganisms CCM, Brno, Czech Republic) was cultivated in solid or liquid medium (potato-dextrose agar - PDA/potato-dextrose broth - PDB) [2% glucose; 20% potato extract; pH 5.6; PDA – addition of 2% agar] (Schau, 1986). Spores were isolated after two weeks of cultivation on PDA at 25 ± 1 °C. Enteroviruses from the *Picornaviridae* family with a genome consisting of single-stranded RNA were used for testing the inhibition effectivity of AgNPs. *Poliovirus* type 1 (vaccine strain), *poliovirus* type 3 (vaccine strain), and *coxsackie* virus A7 effect on cell line were evaluated, and all tested strains share the same median tissue culture infecting dose (TCID<sub>50</sub>).

The RD(A) cell line derived from a malignant embryonal rhabdomyosarcoma (ATCC CCL 136 RD- *Rhabdomyosarcoma*, embryonal, human) cultured in Eagle's minimal essential medium with L-glutamine (WHO/EPI/CDS/POLIO/90.1) was used to determine the antiviral effect. TCID<sub>50</sub> represented a dilution of 10<sup>-9</sup> virus particles. TCID<sub>50</sub> was determined based on the Kärber equation (Kärber, 1931). The cell suspension with a concentration of 1.2 x 10<sup>8</sup> cells.dm<sup>-3</sup>. The Fetal Bovine Serum (5%) was used as a growth factor in the culture medium, with 1 mol.dm<sup>-3</sup> HEPES (in 0.85% NaCl) (pH 7.0) as a buffer system, with the addition of antibiotics, penicillin and streptomycin (1 x 10<sup>-7</sup> g.dm<sup>-3</sup>).

### Growth curve and inhibition of bacterial growth

The prepared suspension of *E. coli* cells (0.5 MFU) was inoculated into a 96-well flat-bottom microtiter plate in a final volume of 300 µl and a final bacterial concentration of 1.5 x 10<sup>9</sup> cells.dm<sup>-3</sup>. Tested AgNPs samples immobilized on 5 x 8 x 0.5 mm silica plates and 5 x 8 x 0.5 mm control silica plates without AgNPs were transferred into a 96-well microtiter plate (1 silica plate for one well).

The growth curve of *E. coli* was designed based on data from the measurement of optical density OD<sub>600</sub> at the start of the experiment and each subsequent hour, with the final measurement at 8 hours. The experiment was realized in three biological replicates, and mean values with standard deviations were calculated. The control sample (pure silica plate) was compared to AgNPs material with the highest Ag at. % (Ag5 - 57%).

Experiments aimed at evaluating the inhibition effectivity of AgNPs immobilized on 5 x 8 x 0.5 mm silica plates were carried out in three biological replicates. The increase of biomass was compared between all tested materials, and the pure silica plate was again used as control. The experiment was realized in four biological replicates, and mean values with standard deviation were calculated. Inhibition effectivity was calculated according to the formula.

$$\text{Inhibition effectivity [\%]} = 100 - \frac{OD_{600} \text{ sample} \times 100}{OD_{600} \text{ control}}$$

### Live/death bacterial cell staining

Detection of live and dead bacterial cells was performed by two independent methods, the modified protocol of Franke et al. (2019) based on the detection of erythrosin B signal and the commercially available kit "LIVE/DEAD™ BacLight™ Bacterial Viability Kit" (Thermo Fisher Scientific, Waltham, USA) according to the manual.

Before erythrosin B detection of live and dead cells, a standard curve from known percentages of live and dead *E. coli* cells was prepared (100% live cells; 75% live/25% dead cells; 50% live/50% dead cells; 25% live/75% dead cells and 100% dead cells). Signal from 100% live and 100% dead cells without erythrosin B was subtracted from readings with stain. Overnight *E. coli* culture was transferred into fresh LB and cultivated until OD<sub>600</sub> 0.08 – 0.12 (0.5 MFU). After the collection of cells, the supernatant was discarded, and cells were resuspended in the same volume of 0.9% NaCl solution [H<sub>2</sub>O (B. Braun Konzern Medical, Bratislava, Slovakia), 0.9% (w/v) NaCl]. Resuspended cells were cultivated for 16 hours with an AgNPs sample, and 100 µl of culture was mixed with 100 µl 0.8% (w/v) erythrosin B in 0.1 mol.dm<sup>-3</sup> Tris, pH 7.5. The suspension was incubated at laboratory temperature for 5 min and centrifugated for 10 min at 10 000 rpm. The supernatant was removed, and the cell pellet was resuspended in 100 µl PBS [0.137 mol.dm<sup>-3</sup> NaCl; 2.7 x 10<sup>-3</sup> mol.dm<sup>-3</sup> KCl; 1 x 10<sup>-3</sup> mol.dm<sup>-3</sup> Na<sub>2</sub>HPO<sub>4</sub>; 1.2 x 10<sup>-3</sup> mol.dm<sup>-3</sup> KH<sub>2</sub>PO<sub>4</sub>; pH 7.4], centrifugated and washed again in PBS. Collected and washed pellet was resuspended in 100 µl PBS and transferred into a 96-well flat bottom microtiter plate, and absorbance A<sub>530</sub> was measured on Synergy H1™ Hybrid Multi-Mode Microplate Reader (BioTek Instruments, Winooski, USA). Standard curves for both detection methods of live and dead cells were constructed based on the mean values of 4 biological replicates, and sample analyses were performed in three biological replicates.

### Inhibition of fungal growth

The antifungal assay was performed by a modified protocol of Broekaert et al. (1990). Spores were isolated from 14 – days old plate cultures into 2 ml of sterile ddH<sub>2</sub>O. Water was pipetted on the mycelia and surface was gently washed. Supernatant was collected and filtered with sterile miracloth (Sigma-Aldrich Production GmbH, Switzerland) into 2 ml sterile tubes. Spores were counted in Thoma cell-counting chamber under Leica TCS SP5 laser scanning confocal microscope (Leica Microsystems, Wetzlar, Germany). Isolated spores of *T. harzianum* were diluted to the final concentration of 10<sup>8</sup> spores.dm<sup>-3</sup> in PDB and transferred into 96-well flat bottom microtiter plate with tested AgNPs samples immobilized on 5 x 8 x 0.5 mm silica plates, or with 5 x 8 x 0.5 mm silica plates without AgNPs. The cultivation was performed at 25 ± 1 °C for 18 hours. After cultivation, absorbance A<sub>595</sub> was measured on Synergy H1™ Hybrid Multi-Mode Microplate Reader (BioTek Instruments, Winooski, USA), and inhibition effectivity was calculated by the formula used for bacterial inhibition. Analyses were performed in three biological replicates, and mean values with standard deviation were calculated.

### Inhibition of virus effect on cells

The suspension of virus particles was pre-treated with AgNPs (samples Ag1, Ag5, and Ag6 - the coatings were applied to silica plates with a size of 5 x 8 x 0.5 mm) in different time intervals - 30, 60, and 90 min, at laboratory temperature.

The virus suspension was inoculated onto a 24-hour monolayer of cell cultures. The cell culture was cultured on slanted culture tubes in an inclined stand at a 5 ° angle, with the flat culture side down. Before inoculation, the growth medium (5% fetal bovine serum – FBS) was replaced with the maintenance medium (2% FBS). The inoculated test tubes were cultured at 36 ± 0.5 °C in a biological incubator with an atmosphere of 5% CO<sub>2</sub>, for at least five days in the first passage and subsequently in the second passage.

Between the passages, the test tubes were monitored until the following passage, and the test tubes from the previous cultivation were kept at a temperature of -20 °C ± 3 °C. A negative control (RD(A) cell monolayer in a medium without viruses) and a positive control were included for each cell culture in the presence of a virus suspension. The images were acquired using an inverted Leica DM IL microscope (Leica Microsystems, Wetzlar, Germany).

### ICP-OES Analysis

AgNPs immobilized on silica plates were incubated in 200 µl LB for 3 hours with shaking at 180 rpm. After the cultivation, silica plates were removed, samples were diluted to a final volume of 5 ml LB, and HNO<sub>3</sub> to a final concentration of 5% (v/v) was added. Determination of Ag concentration in tested samples was measured on an optical emission spectrophotometer ICP Thermo ICAP 7000 Dual (Thermo Fisher Scientific, Waltham, Massachusetts, USA) with inductively coupled plasma. Analysis parameters are included in Table 2. The standard silver solution (Sigma-Aldrich Production GmbH, Switzerland) was used for the calibration, with silver concentrations 4.97 x 10<sup>-2</sup> g.dm<sup>-3</sup>; 4.97 x 10<sup>-3</sup> g.dm<sup>-3</sup>; 4.97 x 10<sup>-4</sup> g.dm<sup>-3</sup>; and 4.97 x 10<sup>-5</sup> g.dm<sup>-3</sup>. The silver concentration in

analyzed samples was automatically calculated based on data from the calibration curve.

**Table 2** ICP-OES analysis parameters

Analysis parameter	Plasma RF Power	Purge Gas Flow	Auxiliary Gas Flow	Coolant Gas Flow	Nebulizer Gas Flow	Nebulizer Gas Pressure	Pump Speed
Value	1150 W	Normal	0.50 dm <sup>3</sup> .min <sup>-1</sup>	12 dm <sup>3</sup> .min <sup>-1</sup>	0.40 dm <sup>3</sup> .min <sup>-1</sup>	120 kPa	50 rpm

**Statistical analysis**

The obtained data were statistically analyzed by the one-way ANOVA test and the Tukey multiple comparisons test using GraphPad Prism, version 8.0.2 (263). Probability values less than 0.05 (p < 0.05) were considered significant. Probability values less than 0.001 (p < 0.001) are displayed if possible.

**RESULTS AND DISCUSSION**

**Effect of silver nanoparticles on the growth curve of E. coli**

Growth of the gram-negative bacteria *E. coli* in the presence of AgNPs immobilized on a 5 x 8 x 0.5 mm silica plate was compared to the growth curve of bacteria in presence of a silica plate without AgNPs by measuring optical density at 600 nm. The effect of AgNPs was evaluated for the lag and exponential phases of growth. *E. coli* growth with silica plate without immobilized AgNPs reached

exponential phase rapidly after 2 hours. If cells were exposed to AgNPs from a silica plate, the lag phase was prolonged for 4 hours (Figure 1). The total percentage of live and dead cells in the presence of AgNPs and confirmation of elongated lag phase suggest efficient antibacterial activity of tested forms of immobilized AgNPs. The inhibition effect on the growth of *E. coli* exceeds IC50 values in all tested materials (Table 3).

Two independent methods for counting live/dead cells percentages were used, with no significant difference depending on the method used. The exponential growth phase in presence of AgNPs was shifted because of the long lag phase, therefore AgNPs are the critical factor that affects the time for preparing the bacteria for new conditions in media. The biomass increase balanced out after 7 hours of cultivation, suggesting that the maximum specific growth rate of *E. coli* is unaffected by AgNPs. The prolongation of the lag phase is reported by other studies (Haque et al., 2017; Li et al., 2010). Dead cell percentages confirmed the lethal effect of AgNPs on gram-negative *E. coli*.

**Table 3** LIVE/DEAD™ BacLight™ Bacterial Viability Kit and erythrosin B evaluation of live and dead cells in presence of AgNPs

Sample composite	LIVE/DEAD™ BacLight™ Bacterial Viability Kit			erythrosin B		
	G/R ratio	live [%]	dead [%]	Average A <sub>530</sub>	live [%]	dead [%]
Ag-TiB <sub>2</sub> 50W	0.649	26.7	73.3	0.643	28.0	72.0
Ag-TiB <sub>2</sub> 100W	0.743	33.4	66.6	0.601	34.0	66.0
Ag-TiB <sub>2</sub> 200W	0.796	37.2	62.8	0.588	35.9	64.1
Ag1	0.587	22.3	77.7	0.671	23.9	76.1
Ag5	0.725	32.1	67.9	0.599	34.3	65.7
Ag6	0.851	41.0	59.0	0.541	42.8	57.2

**Legend:** G/R ratio – the ratio of green and red fluorescence signal, Average A<sub>530</sub> – average value of three biological replicates

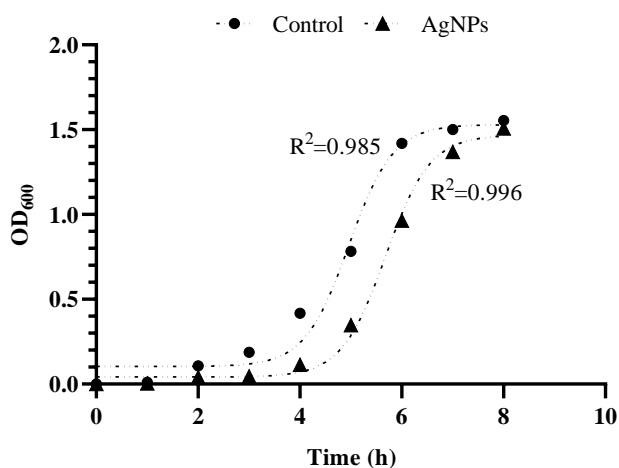


**Figure 1** Effect of silver nanoparticles (sample Ag5) on the growth curve of *E. coli*

**AgNPs effect on biomass growth of E. coli**

Based on the strong inhibitory effect of AgNPs confirmed by live/dead cell count and lag phase shifting, the next objective was to evaluate a possible relationship between the concentration of immobilized or released AgNPs from silica matrix and the inhibition of biomass increase of *E. coli*. Data for atomic percent of silver in tested material were already available (Table 1), and measurement of released silver ions and AgNPs was performed by ICP-OES (Figure 2). Silver concentration in cultivation media was, as expected, dependent on the initial atomic percentage in the tested material (Anekthirakun and Imyim, 2019). In general, tested samples produced by physical vapor deposition (AgTiB<sub>2</sub>) released more silver than samples prepared by high target utilization sputtering (Ag1, Ag5, Ag6), although atomic percentages are higher in the case of HiTUS samples. When the effect on biomass growth is evaluated, HiTUS representatives reached 65.8% (Ag6), 67.1% (Ag1), and 71% (Ag5) inhibition; PVD samples caused 59.2% (AgTiB<sub>2</sub> 100W), 71.1% (AgTiB<sub>2</sub> 50W), and 76.2% (AgTiB<sub>2</sub> 200W) inhibition. Differences between

samples are statistically significant, but a small range of evaluated inhibition is an assumption that other factors (environmental, mechanical) can be considered for possible future use in a wide range of applications.

The Ag6 sample released a relatively low amount of Ag in media from the immobilized matrix (4.7 x 10<sup>-4</sup> g.dm<sup>-3</sup>) but kept the inhibitory effect at 65%. The highest amount of released Ag was detected in AgTiB<sub>2</sub> 200W (1.295 x 10<sup>-3</sup> g.dm<sup>-3</sup>), corresponding with the highest inhibitory effect of 76%. Published studies about the inhibitory effect of AgNPs in soluble form suggest a concentration of 1 x 10<sup>-2</sup> – 4 x 10<sup>-2</sup> g.dm<sup>-3</sup> for the total suppression of bacterial growth (Haque et al., 2017; Wei et al., 2019). Detection of the strong inhibitory effect of tested AgNP materials suggests that it was not influenced only by the soluble fraction of released Ag ions and nanoparticles but was contributed by available AgNPs in immobilized form (He et al., 2021).

Several studies suggest AgNPs inhibitory effect dependency on the electrostatic interaction with cell wall lipopolysaccharides of gram-negative bacteria (Abadeer et al., 2015; El Badawy et al., 2011; Jacobson et al., 2015). The significant effect of AgNPs in an immobilized matrix can be explained by the hypothesis of Pajerski et al. (2019): van der Waals attractive forces and the electrostatic repulsive forces are part of the interaction between bacterial cells and AgNPs in liquid suspension. Moreover, Joshi et al. (2020) suggest the possible dependence of these interactions on the variability of tested bacteria cell wall composition, density, and structure, which can be the main reason for the wide range of minimal inhibitory concentration of Ag published in various studies.

The obtained data on released Ag ions and AgNPs in culture media are valuable indicators for answering questions of environmental safety associated with the increased rate of release of metal nanoparticles in the biosphere. Properties of AgNPs, such as the production of ROS, DNA damage, or inflammation progress in cells, are major potential hazards for living organisms if their concentration is not controlled and regulated (Calderón-Jiménez et al., 2017). Mechanisms of the impact of AgNPs on the environment remain unclear due to the lack of suitable available technologies and the difficulty of monitoring their production (Xu and Zhang, 2018). The main benefit of tested materials with antibacterial properties is a shallow rate of releasing Ag ions or AgNPs in solution during *in vitro* tests, which suggests their great potential for future applications in various fields of industry, pharmacy, or medicine.

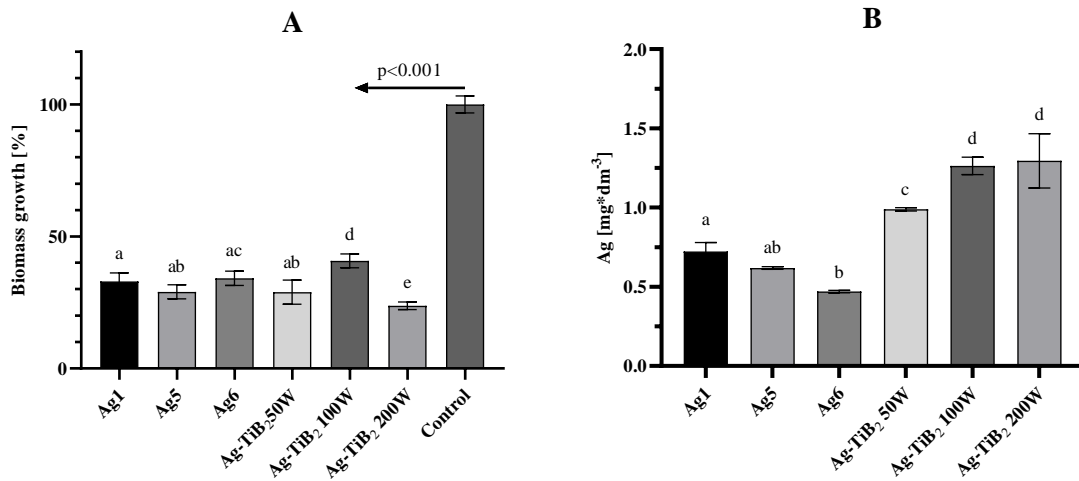


Figure 2 A – Inhibition of *E. coli* growth in presence of AgNPs, B – ICP analysis of Ag content in LB after inhibition test

**Inhibition of *Trichoderma harzianum* growth by AgNPs**

Successful tests aimed at bacterial growth inhibition open questions about possible growth inhibition or suppression of another group of pathogenic microscopic organisms, microscopic filamentous fungi. AgNPs from all tested materials exhibited a significant inhibition effect ( $p < 0.001$ ) on the biomass growth of *T. harzianum*. AgNP samples prepared by HiTUS showed a more substantial inhibition effect than AgNPs prepared by PVD, and the inhibition effect was directly dependent on at. % Ag in the sample. The most potent inhibition effect was measured in Ag5, which reduced the growth of *T. harzianum* by 68.8%, followed by Ag1 (57.5%), AgTiB<sub>2</sub> 200W (49.6%), Ag6 (40.8%), AgTiB<sub>2</sub> 100W (37.9%), and AgTiB<sub>2</sub> 50W (16.1%) (Figure 3).

Mechanisms of AgNPs effectiveness on growth suppression are not well characterized, few published reports suggest possible factors influencing cells on either molecular or physiological levels, namely cell wall degradation and changes in enzyme activities (Ameen et al., 2021; Du et al., 2020). Zarowska et al. (2019) defined  $1.07 \times 10^{-2} \text{ g.dm}^{-3}$  AgNPs concentration as inhibitory for *Paecilomyces variotii*, *Chaetomium globosum*, *Aspergillus brasiliensis*, *Penicillium pinophilum*, and *Trichoderma virens*. Lag phase duration increased up to 10 times, and final optical density in the presence of AgNPs decreased more than 36 folds. Our results confirmed the lower optical density of *T. harzianum* biomass caused by the AgNPs effect, inhibition levels published for *T. virens* (18%) are comparable with AgTiB<sub>2</sub> 50W (16.1%). Inhibition effectivity of AgNPs is in the case of filamentous fungi highly dependent on species, nanomaterial properties (size, shape, capping agent), and concentrations of Ag, where inhibition effect is evident within the order of magnitude about  $1 \times 10^{-2} \text{ g.dm}^{-3}$  Ag (Vazquez-Muñoz et al., 2017).

**Effect of AgNPs on infectivity**

AgNPs samples prepared by PVD (Ag1, Ag5, Ag6) were tested for their possible inhibitory or lethal effect on three strains of single-strained RNA viruses, poliovirus type 1, poliovirus type 3, and coxsackie virus A7, in the course of two passages. Our testing proves that after pre-treatment of virus suspension with AgNPs for 30, 60, and 90 min, no detectable infection of RD(A) cell monolayers in the first passage was observed. However, the coxsackie virus A7 infection was detected on cell monolayers from the second passage when the time of pre-treatment of the virus with AgNPs was 30 min (not presented). In the case of 90 min virus suspension pre-treatment with AgNPs no infection appeared on cell monolayers (second passage) (Figure 4F, G, H). When infected monolayers of RD(A) cells (Figure 4B, C, D) are compared to cells infected with 90 min AgNP pre-treated virus suspension, there is clear evidence of virus inhibition. On the other hand, no adverse effect of AgNPs on cell monolayers during this time is observed (Figure 4E), and the cell viability was the same as control (Figure 4A). The previous study (Thuc et al., 2016) confirmed the effect of AgNPs against poliovirus-infected human rhabdomyosarcoma RD(A) cells. Similar to our findings, AgNPs had no cytopathic effect on RD cells up to  $0.1 \text{ g.dm}^{-3}$ .

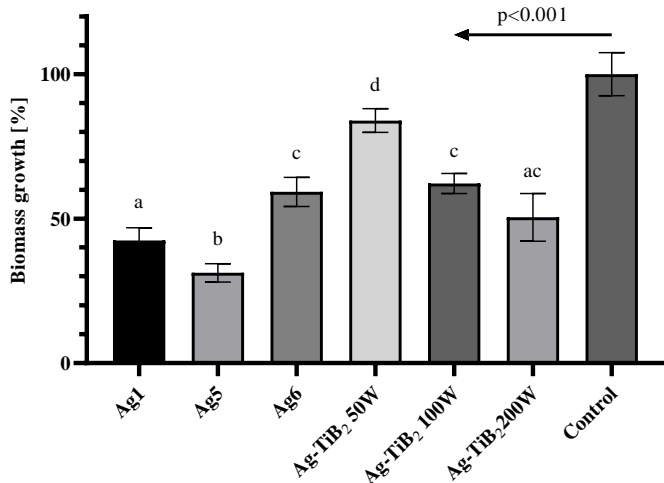


Figure 3 AgNPs effect on the biomass growth of *Trichoderma harzianum*

Table 4 Time course of the virus pre-treatment assay

	First passage			Second passage		
	30 min	60 min	90 min	30 min	60 min	90 min
The exposure time of viruses to AgNPs						
<i>Poliovirus</i> type 1	-	-	-	-	-	-
<i>Poliovirus</i> type 3	-	-	-	-	-	-
<i>Coxsackie</i> virus A7	-	-	-	+	-	-

Legend: “+” – formation of cytopathic effect (CPE), without Ag inhibitory effect; “-” – no detectable CPE, with Ag inhibitory effect

To date, the effect of 31 viruses belonging to 17 different virus families was reduced by AgNPs. In general, the antiviral effect of AgNPs is influenced by the dimension of particles, and the effect is directly dependent on concentration and exposure time (Luceri et al., 2023), which corresponds with our findings that resulted in infection with 30 min pre-treated coxsackie virus A7. Jeremiah et al. (2020) reported the potent antiviral effect of AgNPs on SARS-CoV-2, which is also a single-stranded RNA virus, thus opening new application possibilities.

AgNPs produced by *Aspergillus terreus* BA6 (“green synthesis of AgNP”) were not able to inhibit the coxsackie B virus, even at the concentration of  $4.38 \times 10^{-2} \text{ g.dm}^{-3}$  (Lotfy et al., 2021), which may be an indicator of increased resistance to the silver of coxsackie viruses.

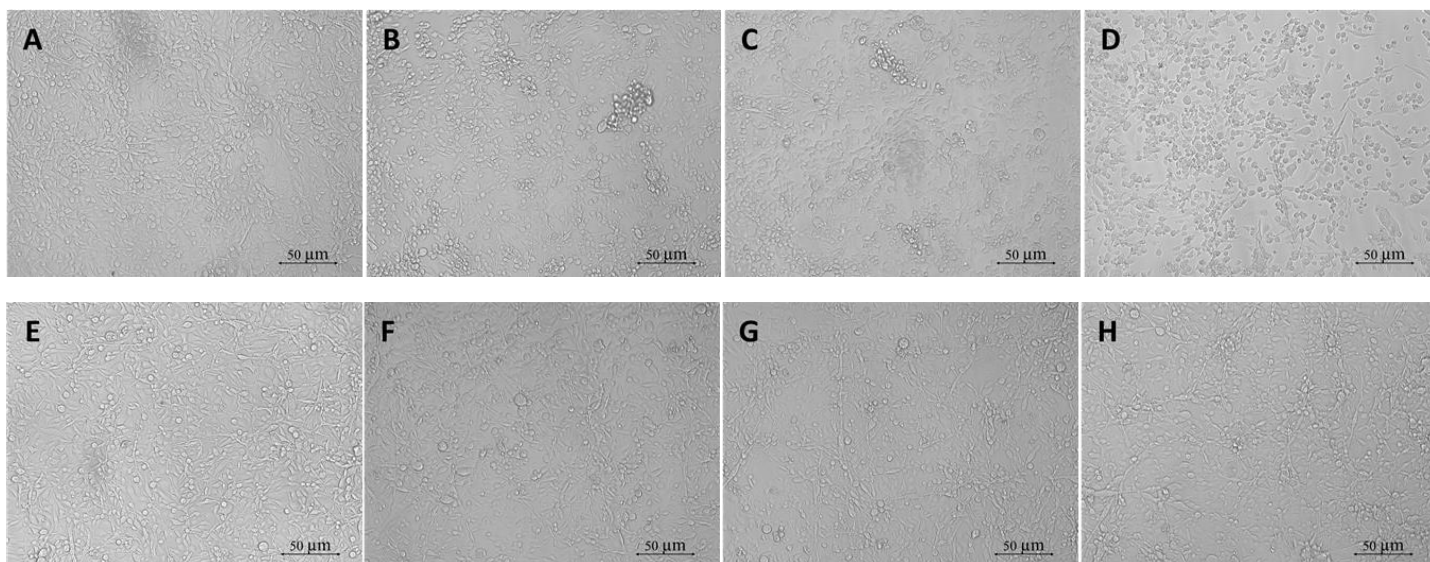


**Figure 4** Results from RD(A) cell monolayer culture infection. **A** – control: the vital monolayer of the RD cell culture in the absence of viruses and AgNPs; **B** - the infected cell monolayer after the exposition by poliovirus type 1; **C** - the infected cell monolayer after the exposition by poliovirus type 3; **D** - the infected cell monolayer after the exposition by coxsackie virus A7; **E** - control: the vital monolayer of the RD cell culture in the absence of viruses, in the presence of AgNPs (AgNP CPE, control); **F** - the infected cell monolayer after the exposition by poliovirus type 1 pre-treated with AgNPs for 90 min.; **G** - the infected cell monolayer after the exposition by poliovirus type 3 pre-treated with AgNPs for 90 min.; **H** - the infected cell monolayer after the exposition by coxsackie virus A7 pre-treated with AgNPs for 90 min.

## CONCLUSION

AgNPs produced by two different methods, HiTUS (Ag1; Ag5; Ag6) and PVD (Ag-TiB<sub>2</sub>-50W; Ag-TiB<sub>2</sub>-100W; Ag-TiB<sub>2</sub>-200W), were tested for their possible antimicrobial effect against model organisms of bacteria (*E. coli*), microscopic filamentous fungi (*T. harzianum*) and viruses (poliovirus type 1; poliovirus type 3; and coxsackie virus A7). Both series of tested materials revealed significantly strong inhibition capabilities on tested microorganisms. An interesting fact is even when the concentration of Ag in liquid media after 3 hours is lower than  $1.5 \times 10^{-3} \text{ g} \cdot \text{dm}^{-3}$ , the inhibitory effect on the growth of *E. coli* is comparable with the results of other authors, who worked with higher Ag concentrations, what suggests the strong inhibitory effect of AgNPs immobilized in the coating of silica plates. *T. harzianum* was susceptible to the inhibitory effect of AgNPs, and the HiTUS sample series showed higher biomass growth inhibition, in general. All three species of viruses were completely inhibited when 60 min or more pre-treatment with HiTUS AgNPs was used. Coxsackie virus A7 could infect RD(A) cells after 30 min pre-treatment, but after 60 mins and more, there was no detectable infection of cells. Obtained results, emphasizing a very low concentration of silver detected by ICP-OES analysis in culture media, open possible applications in various fields, especially when the concentration of released Ag must be held under a low threshold. Analysed materials may represent an environmental safely and effective tool for inhibition of microorganisms.

**Acknowledgments:** This publication was created with the support of the Operational Program Integrated Infrastructure for the project: Development of nanostructured coatings with inactivating effect on viruses and bacteria for different types of flexible materials, ITMS: 313011AUH4, co-financed by the European Regional Development Fund.

## REFERENCES

- Abadeer, N. S., Fulop, G., Chen, S., Kall, M., and Murphy, C. J. (2015). Interactions of bacterial lipopolysaccharides with gold nanorod surfaces investigated by refractometric sensing. *ACS Applied Materials & Interfaces*, 7(44), 24915–24925. <https://doi.org/10.1021/acsami.5b08440>
- Ameen, F., Alsamhary, K., Alabdullatif, J. A., and ALNadhari, S. (2021). A review on metal-based nanoparticles and their toxicity to beneficial soil bacteria and fungi. *Ecotoxicology and Environmental Safety*, 213, 112–127. <https://doi.org/10.1016/j.ecoenv.2021.112027>
- Anees Ahmad, S., Sachi Das, S., Khatoun, A., Tahir Ansari, M., Afzal, M., Saquib Hasnain, M., and Kumar Nayak, A. (2020). Bactericidal activity of silver nanoparticles: A mechanistic review. *Materials Science for Energy Technologies*, 3, 756–769. <https://doi.org/10.1016/j.mset.2020.09.002>
- Anekthirakun, P., and Imyim, A. (2019). Separation of silver ions and silver nanoparticles by silica based-solid phase extraction prior to ICP-OES determination. *Microchemical Journal*, 145, 470–475. <https://doi.org/10.1016/j.microc.2018.11.008>
- Balagna, C., Perero, S., Percivalle, E., Nepita, E. V., and Ferraris, M. (2020). Virucidal effect against coronavirus SARS-CoV-2 of a silver nanocluster/silica composite sputtered coating. *Open Ceramics*, 1, 100006. <https://doi.org/10.1016/j.oceram.2020.100006>
- Broekaert, W. F., Terras, F. R. G., Cammue, B. P. A., and Vanderleyden, J. (1990).

- An automated quantitative assay for fungal growth inhibition. *FEMS Microbiology Letters*, 69(1–2), 55–59. <https://doi.org/10.1111/j.1574-6968.1990.tb04174.x>
- Calderón-Jiménez, B., Johnson, M. E., Montoro Bustos, A. R., Murphy, K. E., Winchester, M. R., and Vega Baudrit, J. R. (2017). Silver nanoparticles: Technological advances, societal impacts, and metrological challenges. *Frontiers in Chemistry*, 5(6). <https://doi.org/10.3389/fchem.2017.00006>
- Cao, Jin, R., and Mirkin, C. A. (2001). DNA-Modified Core-Shell Ag/Au Nanoparticles. *Journal of the American Chemical Society*, 123(32), 7961–7962. <https://doi.org/10.1021/ja011342n>
- Carlson, C., Hussain, S. M., Schrand, A. M., K. Braydich-Stolle, L., Hess, K. L., Jones, R. L., and Schlager, J. J. (2008). Unique Cellular Interaction of Silver Nanoparticles: Size-Dependent Generation of Reactive Oxygen Species. *The Journal of Physical Chemistry B*, 112(43), 13608–13619. <https://doi.org/10.1021/jp712087m>
- Dorobantu, L. S., Fallone, C., Noble, A. J., Veinot, J., Ma, G., Goss, G. G., and Burrell, R. E. (2015). Toxicity of silver nanoparticles against bacteria, yeast, and algae. *Journal of Nanoparticle Research*, 17(4), 172. <https://doi.org/10.1007/s11051-015-2984-7>
- Du, J., Zhang, Y., Yin, Y., Zhang, J., Ma, H., Li, K., and Wan, N. (2020). Do environmental concentrations of zinc oxide nanoparticle pose ecotoxicological risk to aquatic fungi associated with leaf litter decomposition? *Water Research*, 178, 115840. <https://doi.org/10.1016/j.watres.2020.115840>
- El Badawy, A. M., Silva, R. G., Morris, B., Scheckel, K. G., Suidan, M. T., and Tolaymat, T. M. (2011). Surface charge-dependent toxicity of silver nanoparticles. *Environmental Science & Technology*, 45(1), 283–287. <https://doi.org/10.1021/es1034188>
- Franke, J. D., Braverman, A. L., Cunningham, A. M., Eberhard, E. E., and Perry, G. A. (2019). Erythrosin B: a versatile colorimetric and fluorescent vital dye for bacteria. *BioTechniques*, 68(1), 7–13. <https://doi.org/10.2144/btn-2019-0066>
- Fubini, B., Fenoglio, I., Tomatis, M., and Turci, F. (2011). Effect of chemical composition and state of the surface on the toxic response to high aspect ratio nanomaterials. *Nanomedicine*, 6(5), 899–920. <https://doi.org/10.2217/nmm.11.80>
- Haque, M. A., Imamura, R., Brown, G. A., Krishnamurthi, V. R., Niyonshuti, I. I., Marcelle, T., Mathurin, L. E., Chen, J., and Wang, Y. (2017). An experiment-based model quantifying antimicrobial activity of silver nanoparticles on *Escherichia coli*. *RSC Advances*, 7(89), 56173–56182. <https://doi.org/10.1039/C7RA10495B>
- He, Y., Li, H., Fei, X., and Peng, L. (2021). Carboxymethyl cellulose/cellulose nanocrystals immobilized silver nanoparticles as an effective coating to improve barrier and antibacterial properties of paper for food packaging applications. *Carbohydrate Polymers*, 252, 117156. <https://doi.org/10.1016/j.carbpol.2020.117156>
- Immunization, W. H. O. E. P. on, and Diseases, W. H. O. D. of C. (n.d.). Manual for the virological investigation of poliomyelitis. World Health Organization. <https://apps.who.int/iris/handle/10665/62186>
- Izai, V., Fiantok, T., Vidiš, M., Truchlý, M., Satrapinskyy, L., Nagy, Š., Roch, T., Turinčová, V., Kúš, P., and Mikula, M. (2023). Structure and chemical composition of thin-film nanocomposites based on silver in organosilicon amorphous matrix prepared by High Target Utilization Sputtering. *Thin Solid Films*, 765, 139643. <https://doi.org/10.1016/j.tsf.2022.139643>
- Jacobson, K. H., Gunsolus, I. L., Kuech, T. R., Troiano, J. M., Melby, E. S., Lohse, S. E., Hu, D., Chrisler, W. B., Murphy, C. J., and Orr, G. (2015). Lipopolysaccharide density and structure govern the extent and distance of

- nanoparticle interaction with actual and model bacterial outer membranes. *Environmental Science & Technology*, 49(17), 10642–10650. <https://doi.org/10.1021/acs.est.5b01841>
- Jadoun, S., Chauhan, N. P. S., Zarrintaj, P., Barani, M., Varma, R. S., Chinnam, S., and Rahdar, A. (2022). Synthesis of nanoparticles using microorganisms and their applications: a review. *Environmental Chemistry Letters*, 20(5), 3153–3197. <https://doi.org/10.1007/s10311-022-01444-7>
- Jeremiah, S. S., Miyakawa, K., Morita, T., Yamaoka, Y., and Ryo, A. (2020). Potent antiviral effect of silver nanoparticles on SARS-CoV-2. *Biochemical and Biophysical Research Communications*, 533(1), 195–200. <https://doi.org/10.1016/j.bbrc.2020.09.018>
- Joshi, A. S., Singh, P., and Mijakovic, I. (2020). Interactions of gold and silver nanoparticles with bacterial biofilms: Molecular interactions behind inhibition and resistance. *International Journal of Molecular Sciences*, 21(20), 7658. <https://doi.org/10.3390/ijms21207658>
- Kalwar, K., and Shan, D. (2018). Antimicrobial effect of silver nanoparticles (AgNPs) and their mechanism – a mini review. *Micro & Nano Letters*, 13(3), 277–280. <https://doi.org/10.1049/mnl.2017.0648>
- Kärber, G. (1931). Beitrag zur kollektiven Behandlung pharmakologischer Reihenversuche. *Naunyn-Schmiedeberg's Archiv Für Experimentelle Pathologie Und Pharmakologie*, 162, 480–483.
- Li, W.-R., Xie, X.-B., Shi, Q.-S., Zeng, H.-Y., OU-Yang, Y.-S., and Chen, Y.-B. (2010). Antibacterial activity and mechanism of silver nanoparticles on *Escherichia coli*. *Applied Microbiology and Biotechnology*, 85(4), 1115–1122. <https://doi.org/10.1007/s00253-009-2159-5>
- Liao, C., Li, Y., and Tjong, S. C. (2019). Bactericidal and cytotoxic properties of silver nanoparticles. *International Journal of Molecular Sciences*, 20(2), 449. <https://doi.org/10.3390/ijms20020449>
- Lotfy, W. A., Alkersh, B. M., Sabry, S. A., and Ghozlan, H. A. (2021). Biosynthesis of Silver Nanoparticles by *Aspergillus terreus*: Characterization, Optimization, and Biological Activities. In *Frontiers in Bioengineering and Biotechnology*, 9. <https://doi.org/10.3389/fbioe.2021.633468>
- Luceri, A., Francese, R., Lembo, D., Ferraris, M., and Balagna, C. (2023). Silver Nanoparticles: Review of Antiviral Properties, Mechanism of Action and Applications. In *Microorganisms*, 11(3). <https://doi.org/10.3390/microorganisms11030629>
- MacCormack, T. J., and Goss, G. G. (2008). Identifying and Predicting Biological Risks Associated With Manufactured Nanoparticles in Aquatic Ecosystems. *Journal of Industrial Ecology*, 12(3), 286–296. <https://doi.org/10.1111/j.1530-9290.2008.00041.x>
- Pajerski, W., Ochonska, D., Brzychczy-Wloch, M., Indyka, P., Jarosz, M., Golda-Cepa, M., Sojka, Z., and Kotarba, A. (2019). Attachment efficiency of gold nanoparticles by Gram-positive and Gram-negative bacterial strains governed by surface charges. *Journal of Nanoparticle Research*, 21, 1–12. <https://doi.org/10.1007/s11051-019-4617-z>
- Pareek, V., Gupta, R., and Panwar, J. (2018). Do physico-chemical properties of silver nanoparticles decide their interaction with biological media and bactericidal action? A review. *Materials Science and Engineering: C*, 90, 739–749. <https://doi.org/10.1016/j.msec.2018.04.093>
- Pulit-Prociak, J., and Banach, M. (2016). Silver nanoparticles – a material of the future...? *Open Chemistry*, 14. <https://doi.org/10.1515/chem-2016-0005>
- Schau, H. P. (1986). J. F. MacFaddin, Media for Isolation - Cultivation - Identification - Maintenance of Medical Bacteria, Volume I. XI + 929 S., 163 Abb., 94 Tab. Baltimore, London 1985. Williams and Wilkins. ISBN: 0-683-05316-7. *Journal of Basic Microbiology*, 26, 240.
- Slepička, P., Slepičková Kasálková, N., Siegel, J., Kolská, Z., and Švorčík, V. (2020). Methods of Gold and Silver Nanoparticles Preparation. In *Materials* 13(1). <https://doi.org/10.3390/ma13010001>
- Thuc, D. T., Huy, T. Q., Hoang, L. H., Tien, B. C., Van Chung, P., Thuy, N. T., and Le, A.-T. (2016). Green synthesis of colloidal silver nanoparticles through electrochemical method and their antibacterial activity. *Materials Letters*, 181, 173–177. <https://doi.org/10.1016/j.matlet.2016.06.008>
- Vazquez-Muñoz, R., Borrego, B., Juárez-Moreno, K., García-García, M., Mota Morales, J. D., Bogdanchikova, N., and Huerta-Saquero, A. (2017). Toxicity of silver nanoparticles in biological systems: Does the complexity of biological systems matter? *Toxicology Letters*, 276, 11–20. <https://doi.org/10.1016/j.toxlet.2017.05.007>
- Wei, H. J., Awang, M. S., Dyana, N., Kernain, D., and Bustami, Y. (2019). Evaluation of anti bacteria effects of citrate-reduced silver nanoparticles in *Staphylococcus aureus* and *Escherichia coli*. *Int. J. Res. Pharm. Sci*, 10, 3636–3643. <https://doi.org/10.26452/ijrps.v10i4.1745>
- Woodcock, D. M., Crowther, P. J., Doherty, J., Jefferson, S., DeCruz, E., Noyer-Weidner, M., Smith, S. S., Michael, M. Z., and Graham, M. W. (1989). Quantitative evaluation of *Escherichia coli* host strains for tolerance to cytosine methylation in plasmid and phage recombinants. *Nucleic Acids Research*, 17(9), 3469–3478. <https://doi.org/10.1093/nar/17.9.3469>
- Xu, J. Y., and Zhang, H. (2018). Long-term effects of silver nanoparticles on the abundance and activity of soil microbiome. *J Environ Sci*, 69, 3–4. <https://doi.org/10.1016/j.jes.2018.06.009>
- Żarowska, B., Koźlecki, T., Piegza, M., Jros-Koźlecka, K., and Robak. (2019). New Look on Antifungal Activity of Silver Nanoparticles (AgNPs). *Polish Journal of Microbiology*, 68(4), 515–525. <https://doi.org/10.33073/pjm-2019-051>